Seismic zonation of the Dead Sea Transform Fault area

Kamal Khair ([1]), **George F. Karakaisis** ([2]) **and Eleftheria E. Papadimitriou** ([2])
([1]) *Department of Geology, American University of Beirut, Lebanon*
([2]) *Geophysics Laboratory, Aristotle University of Thessaloniki, Greece*

Abstract
The Dead Sea Transform Fault constitutes the northwestern boundary of the Arabian plate, accommodating the plate's lateral movement relative to the African plate. A complete and homogeneous catalogue of historical earthquakes has been compiled and used in the subdivision of the fault area into the following segments: 1) Araba segment, which extends along Wadi Araba and the southernmost part of the Dead Sea (29.5°-31.3°N) and trends SSW-NNE with scarce historical and instrumental seismicity; 2) Jordan-valley segment, which extends along the central and northern parts of the Dead Sea and the Jordan valley to the Huleh depression (31.3°-33.1°N) and trends S-N with moderate historical seismicity; 3) Beqa'a segment, which extends along the western margin of the Beqa'a valley in Lebanon (33.1°-34.5°N) and trends SSW-NNE with strong historical seismicity; 4) El-Ghab segment, which extends along the eastern flank of the coastal mountain range of Syria (34.5°-35.8°N) and trends S-N with moderate historical seismicity; 5) Karasu segment, which extends along the Karasu valley in SE Turkey (35.8°-37.3°N) and trends SSW-NNE, exhibiting the strongest historical seismicity of the area. Probabilities for the generation of strong ($M \geq 6.0$) earthquakes in these segments during the next decade are given, by the application of the regional time and magnitude predictable model.

Key words *Eastern Mediterranean – Dead Sea Transform Fault – historical seismicity – seismic zonation – probabilities*

1. Introduction

The easternmost Mediterranean region is characterized by low seismicity, at least during the instrumental era. However, this region has suffered from many destructive earthquakes in the past which, from all accounts, have originated along the Dead Sea Transform Fault (DSTF). Being one of the most interesting examples of continental transform faulting in the world, this fault delineates the boundary between the Arabian plate to the east, and the African plate to the west, running roughly from south to north for about 900 km. It extends from the northern tip of the Gulf of Aqaba through Wadi Araba, the Dead Sea, the Jordan valley, the Huleh depression, the Beqa'a valley and the El-Ghab graben to the Karasu valley. At the northern end of this valley, DSTF merges with the East Anatolian fault, which constitutes the boundary between the African and Arabian plates to the south, and the Anatolian plate, to the north (fig. 1).

Geological, geomorphological and geophysical evidence indicate that since the early or middle Miocene the left lateral strike slip motion along DSTF resulted in a relative displacement ranging between 105-110 km in its southern segment and about 60 km in its northern segment (Dubertret, 1932; Quennell, 1959, 1984; Freund *et al.*, 1970; Hancock and Atiya, 1979; Bartov *et al.*, 1980; Garfunkel, 1981; Hatcher

Mailing address: Prof. George F. Karakaisis, Geophysics Laboratory, Aristotle University of Thessaloniki, GR 54006 Thessaloniki, Greece; e-mail: karakais@geo.auth.gr

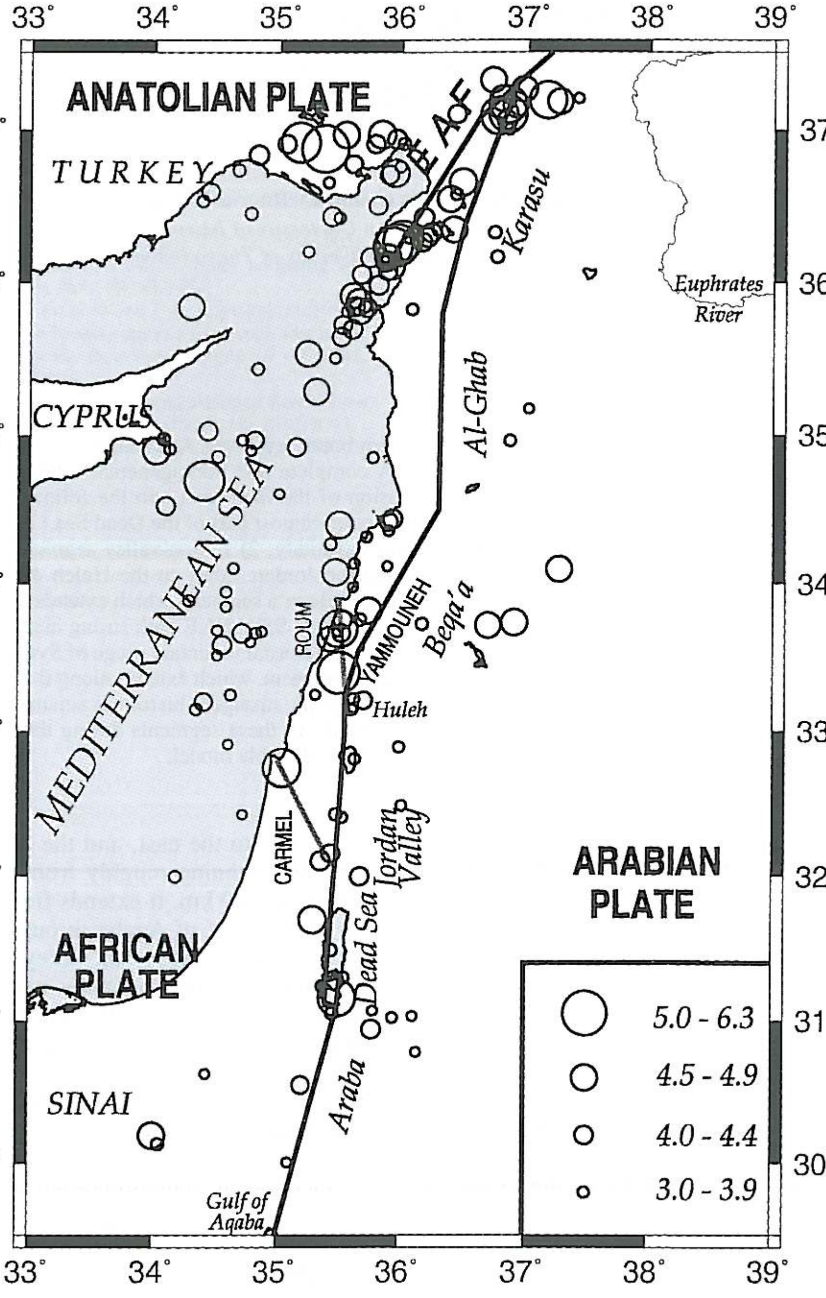

Fig. 1. Map of the Eastern Mediterranean region showing the extension of the Dead Sea Transform Fault and the location of the epicenters of earthquakes with $M \geq 3.0$ (taken from the ISC and NEIC catalogues) that occurred in the past 35 years (1964-1998) in the area between 34° and 38°E meridians. The data can not be considered complete, but they indicate the low seismicity of the area.

et al., 1981; Joffe and Garfunkel, 1987; Girdler, 1990; Chaimov *et al.*, 1990). The average total displacement rate along this fault in the past 20 000 years has been found to be about 6 mm/yr (Zak and Freund, 1966; Freund *et al.*, 1970; Garfunkel and Bartov, 1977; Ben-Menahem, 1981a), while Garfunkel *et al.* (1981) estimated that this rate was only 1.5-3.5 mm/yr in the last 1000-1500 years. Radwan *et al.* (1992) estimated an average rate of about 5 mm/yr of sinistral displacement in the northern segment during upper Pleistocene.

Most of the studies on this area refer to the zone between the Gulf of Aqaba to the Huleh depression as the southern segment and the remaining part to the north as the northern segment (Barazangi *et al.*, 1993; Khair *et al.*, 1997). However, some studies consider the Lebanese part an additional central segment (Butler *et al.*, 1998). Although these subdivisions had some tectonic basis, they were mainly applied for orientation in referring to some areas.

In a series of studies Ben-Menahem (1981a, 1991) defined four segments along DSTF, aiming at rendering the seismicity of each segment more or less uniform. On the other hand, he identified seven segments on the basis of tectonic features only (Ben-Menahem, 1991). Salamon *et al.* (1996) concluded that the DSTF exhibits variable characteristics: along the Yammoneh bend the seismogenic belt is wide, while in the south it narrows and the seismic activity tends to be concentrated in the deep depression of the Dead Sea basin. Further to the south, the seismicity of the Araba segment is very low. Papazachos *et al.* (1997a) divided the DSTF into two seismogenic regions on the basis of the meizoseismal area of the May 20, 1202 earthquake (Ambraseys and Melville, 1988) and of a spatial cluster of strong earthquakes at the Syrian-Turkish borders.

This study analyzes the seismicity reflected in the historical and instrumental records, with a greater emphasis on the first. Based on the geometry, geomorphology, structural geology and historical seismicity of the Dead Sea Transform Fault area, the region has been divided into five seismogenic zones. Moreover, probabilities for the generation of strong mainshocks in these zones during the next ten years are determined.

2. Compilation of the earthquake catalogue

Seismicity studies depend largely on the available information and completeness and reliability of the earthquake catalogue used. In the present study, as far as completeness is concerned, an attempt was made to include all significant earthquakes reported in the literature, even those with inadequate description of focal parameters. As regards the reliability of the data, it needs to be borne in mind that since no primary sources were used but rather published catalogues were reviewed, credit was given to data including all basic focal parameters.

Table I lists all known strong ($M_s \geq 5.9$) earthquakes since 2150 B.C. which occurred in the area of the Dead Sea Transform Fault. In addition, it gives information on earthquakes with magnitudes $M_s \geq 5.5$ for the period 1900-1909, and with $M_s \geq 5.0$ since 1910. The data reviewed in the catalogue were collected from 23 catalogues and individual articles (see table I for references) with the main goal of this task being to include all significant historical earthquakes with magnitudes estimated by the authors of the catalogues and articles on the basis of damage reports found in chronicles. In the case of events for which no magnitude and/or epicenter coordinates were given, their selection was based either on the damage description or whether they have been encountered in other independent sources.

In the cases where different estimates for the same event are given in different sources, preference was given to those sources providing all basic focal parameters. However, in several cases these parameters were adopted from different sources rather than from a single source. This selection was based on the fact that some reliable sources, in terms of date or date and magnitude, do not report other parameters, which could be encountered in other sources. Moreover, some parameters (especially magnitudes) were adopted from sources with values close to the average value of most sources and hence extreme values were mostly discarded. Nevertheless, the last column of table I (references and remarks) gives the source of the adopted values and the discarded ones, the parameter of disagreement and sometimes its value given in the source. Wherever M_L values appear in the table, they were used to calculate the M_S values of magnitude by an equation derived by Ben-Menahem *et al.* (1977). It is worth noting that all M_L values were obtained from studies authored or co-authored by Ben-Menahem (1981a, 1991) and that the most thorough catalogues which incorporate most of the data for this area were compiled by Ambraseys and his colleagues (Ambraseys, 1992, 1997; Ambraseys and Melville, 1988, 1995; Ambraseys and Barazangi, 1989; Ambraseys and Jackson, 1998).

The ambiguous nature of historical seismic records is well reflected in the discrepancies of earthquake parameters found in different sources. This fact requires a skeptic approach in the collection of data in order to remove the uncertainties and build up the data on a solid ground. However, this approach should invite us to blindly ignore events with incomplete data as this might negatively affect our conclusions. Hence, and for the sake of completeness, the table includes events that are listed in other catalogues without assigned coordinates and/or magnitudes.

3. Seismicity of the study area

The slow rate of motion along the DSTF has great impact on the seismicity of the area. The instrumental records in the 20th century show that the region has very low seismicity. Figure 1 shows the epicenters of earthquakes with magnitudes equal to or larger than 3.0 taken from ISC and NEIC bulletins that occurred in the past 35 years (1964-1998) in the broader area of the DSTF (34°-38°E). It can be observed, without claiming completeness for small magnitude earthquakes that, in general, the scarcity of events is obvious, though for the El-Ghab and NE Beqa'a regions it may be artificial due to a lack of recording stations in Syria before 1996. Out of 11 events of magnitude larger than 4.9, three occurred along the East Anatolian Fault and four at the northern end of Karasu. The southwest extension of the East Anatolian Fault into the Cyprus arc is well delineated by a considerable number of earthquakes with varying magnitudes. Moreover, the northern extension of the two leaky fault branches, namely, the Carmel and Roum faults, into the Mediterranean Sea is outlined (fig. 1) (Ben-Menahem and Aboodi, 1981; Shapira and Feldman, 1987; Van Eck and Hofstetter, 1990; Hofstetter *et al.*, 1996; Butler *et al.*, 1997).

As mentioned in the previous paragraph, the lack of recording seismic stations and the short period (35 years) of observation may account for the low background seismicity depicted in fig. 1, since the historical seismic record indicates that the region suffered from many destructive earthquakes in the past 4200 years.

Figure 2a shows a plot of the cumulative number of earthquakes with $M_S \geq 5.9$, which occurred along the DSTF as a function of time. It is observed that few events were reported in the literature before the Christian era while data since 184 B.C. seem to be accumulated rather regularly. Therefore, fig. 2b shows similar plots for different cut-off magnitudes since 200 B.C. It can be seen that there are quiescent periods with duration of a few centuries alternating with periods with high seismic activity which last several decades. If, for instance, earthquakes with $M_S \geq 6.3$ are considered, it emerges that there are three periods with low activity and three periods with high activity, as shown in table II. During the low seismic activity periods, the mean recurrence time, $T_{6.3}$, for earthquakes with $M_S \geq 6.3$, equals 83 ± 20 years, whereas during the high seismic activity periods, $T_{6.3} =$ $= 16 \pm 5$ years. Ambraseys (1989) already identified this pattern in the DSTF as well as in other areas in Middle East (East Anatolian Fault, Zagros). He concluded that deformations associated with earthquakes in these zones seem to occur every few hundred years during relatively short paroxysmal periods of strong events.

Table I shows that in the past 2000 years there have been nine earthquakes of $M_s \geq 7.3$, three of which (551, 1201 and 1759) occurred in Lebanon and the remaining six (115, 245, 859, 1139, 1170 and 1822) in Karasu. This table also shows that the largest earthquake in the area of El-Ghab occurred in 1157 (M_S = 7.2), and that the last relatively strong earthquake (M_S = 6.6) occurred in 1796. Concerning the Jordan valley and the Dead Sea, table I shows that the largest earthquake in the past two millennia occurred in 746 with a surface wave magnitude equal to 7.2.

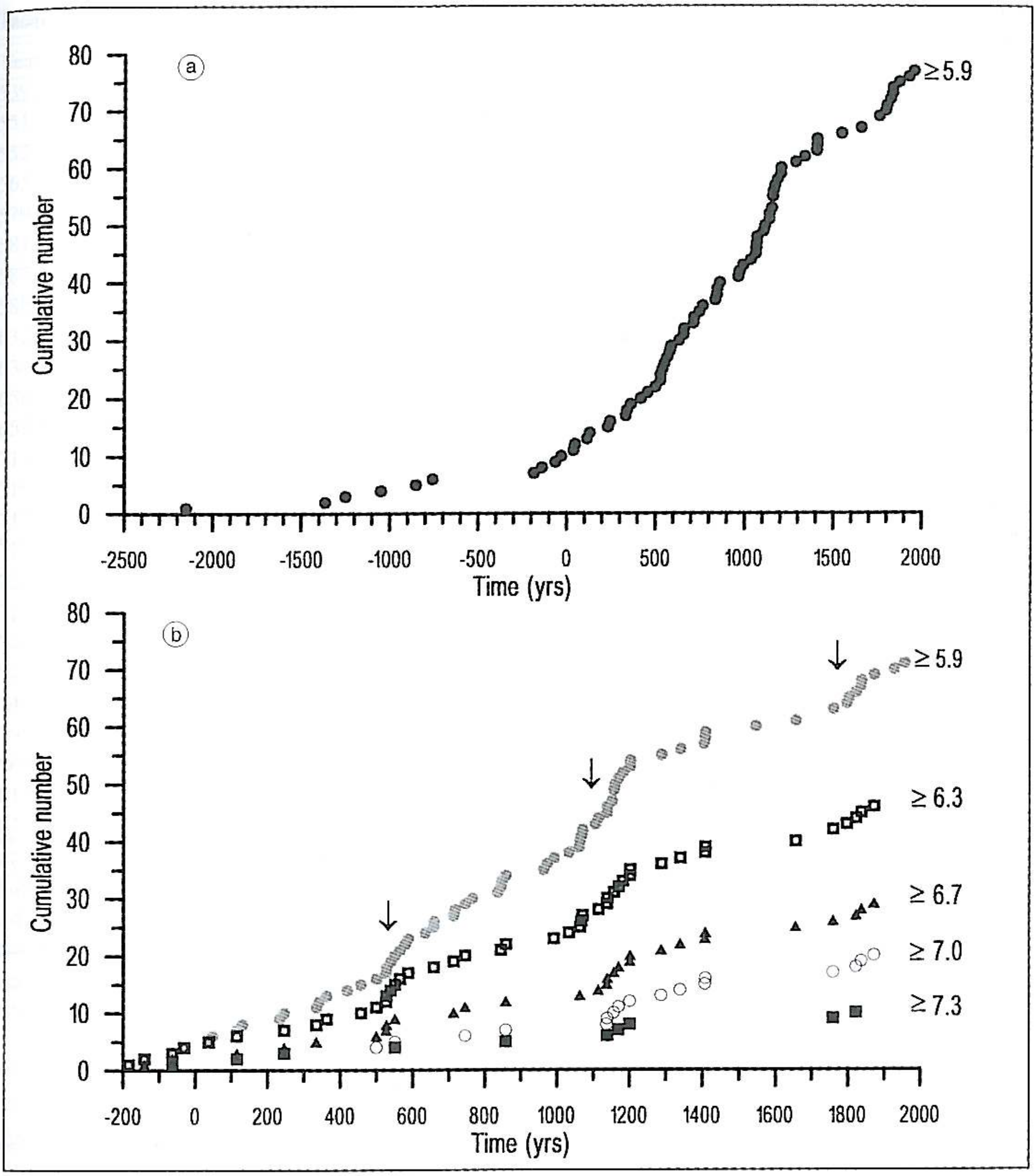

Fig. 2a,b. a) The cumulative number of earthquakes with $M_s \geq 5.9$ as a function of time during 2150 B.C.-1998. Since historical earthquake information seems to be regularly accumulated from about 200 B.C., the cumulative number of earthquakes with M_s equal to or larger than 5.9, 6.3, 6.7, 7.0 and 7.3, respectively, as a function of time during 184 B.C.-1998 is plotted in (b). It is observed that low seismic activity periods alternate with high seismic activity periods, indicated by arrows.

Table I. A catalogue of earthquakes that occurred in the area of the Dead Sea Transform Fault, during the past four millennia.

Year	Zone	Date	Time	M_S	M_L	Lat.	Long.	References and remarks
– 2150	A			7.3		31.1	35.5	N
– 1566	A					31.5	35.3	N
– 1365	G			7.7	7.8			BM,91,79; B; PK(X)
– 1250	J			6.3	6.5	32.0	35.5	BM79,81b; N
– 1050	A			6.0	6.2			BM79 (near Timna)
– 854	J			6.4	6.6			BM79,81b
– 759	B	1011		7.2	7.3	33.2	35.7	BM91,79(Δf = 1200 km), 81b; N; G(-750)
– 199	B							G
– 184	K			6.6	6.8	36.2	36.1	BM79
– 140	K	0221		6.8	7.0			BM79,91; G (-148); PK(VIII)
– 64	K			7.4	7.5	36.2	36.1	BM91,79(Δf > 500 km), 81a; AAT; N(7.0)
– 33	A					31.2	34.2	N 9C
– 31	J	0902		6.5	6.7	32.0	35.5	BM91,79,81a,b; G; PK(VII); AAT(X); N
– 9	A							BM91
37	K	0323		6.3	6.5	36.0	36.0	G(D); BM81a(M); AJ(C)
47	K							G
48	A			6.0	6.2			BM79,81a
52	K					36.1	36.1	N
115	K	1213		7.3	7.4	36.1	36.1	BM79,91,81a; N(C); AJ(≠C); G; PK(VII); AAT
130	B			5.9	6.1			BM79,81a; AAT
233	B			6.1	6.3			BM79,81a
245	K			7.4	7.5			BM79,81a
306	B					33.2	35.1	N
334	K			6.8	7.0			BM79,81a
341	K			6.0	6.2	36.2	36.1	BM81a; N(C); G
348	B					33.9	35.5	N
362	A	0524		6.5	6.7	31.3	35.6	BM91,79,81a,b; N(6.4); G(361); AAT(363)
394	K					36.1	36.1	N 9D
419	A			6.0	6.2	31.2	34.2	BM79,81a; N(C); G; AAT
425	J					31.5	35.1	N
447	J					31.5	35.1	N(C); AAT
450	B							G(450-457)
457	K	0914		6.3	6.5	36.1	36.1	BM81a; N(C); G(458)
494	B					34.5	35.5	N; PK(VIII)
500	K			7.2	7.3	36.2	36.1	BM91,79(Δf = 1100 km), 81a
522	K					36.2	36.1	N
525	K	0900				36.1	36.1	N
526	K	0520		6.8	7.0	36.2	36.1	BM91,81a (6.5); G
528	K	1129		6.9	7.1	36.2	36.1	BM91,79(Δf = 800 km), 81a; G; PT(X-XI); N(7.5)

Table I (*continued*).

Year	Zone	Date	Time	M_S	M_L	Lat.	Long.	References and remarks
539	K	1129		6.6	6.8			G; BM81a (M,532)
551	B	0706		7.5		33.9	35.5	B(M); N(C); G; BM79(7.8L); PK(XI); AAT
557	K	0709				36.1	36.1	N
565	K			6.5	6.7	36.2	36.1	BM79,91(Δf = 850 km); N(C); G(567)
579	K			5.9	6.1			BM81a
581	K					36.1	36.1	N; G(580/81)
587	K	0930		6.3	6.5			BM81a
588	K	1031				36.1	36.1	N; G
632	J							G; AAT
634	K			6.0	6.2			PT(VIII); G; BM81a (639)
658	J	0615		6.4	6.6	32.5	35.5	BM79,81a,b, PK(VIII), AAT
659	J			5.9	6.1			BM81a; G; AAT
713	K	0320		6.8	7.0	36.0	36.0	N(C); BM79,81a; PT(IX); G
716	K	0825				36.0	36.0	N
717	G	1224		5.9	6.1			G; BM81a
718	K	0914						G
722	K	0619						G
723	G	1224						G
746	J	0118	160000	7.2	7.3	32.0	35.5	BM79,91(Δf = 1200 km),81a,b; N; G
748	B	0831				33.5	36.3	N(C); PT(747,IX)
749	B	0118	110000					PT(C); G; PK(748; VII); AAT (X)
758	A					31.2	34.2	N
765	J	0503		6.0	6.2			BM79,81a; G(756)
813	G							G
835	K	0105		5.9	6.1	36.0	36.0	BM81a; N(C); PT(VIII-IX); G
844	B	0918		6.3	6.5	33.5	36.3	BM81a; N(C); G
845	K							PT(IX)
847	B	0400		6.0	6.2	33.5	36.3	BM79,81a; N(C); PT(VIII); G
847	B	1124				33.5	36.3	N
854	J							PT(X-XI)
859	K	0408		7.9	8.0	36.2	36.1	BM79,91(Δf = 1500 km),81a; N; PT(X-XI); G; P; AAT
951	K							PT(VIII-IX)
963	K	0722		6.1	6.3	36.5	37.0	BM81a; N(C); G(Sep 951)
972	K			5.9	6.1	36.1	36.1	PT; BM81a(973); N(C); G
974	B							PT(VIII-IX); G
991	B	0405		6.5	6.7	33.3	36.2	BM91,79(Δf = 500 km),81a; N; PT; G; PK(VII)
995	G							G; PT
1002	B							AAT; PT(IX)
1016	J							AAT
1029	B	0120						PK(VI)

Table I (*continued*).

Year	Zone	Date	Time	M_S	M_L	Lat.	Long.	References and remarks
1033	J	1205		6.5	6.7	32.5	35.5	BM91,79(Δf = 500 km),81b; AJ(C); N(≠C&D); AAT(IX-X)
1060	J			5.9	6.1			BM79,81a
1063	G	0420		6.9	7.1			BM79,81a; B; PK(IX); AAT
1067	A	0420		6.3	6.5			BM79,81a
1068	A	0318				31.8	35.0	N
1070	A	0225		6.3	6.5			BM79,91,81a; AAT
1091	K	0917				36.1	36.1	N(C); PT(IX)
1105	B	1224		5.9	6.1			BM79(Δf = 200 km), 81a; AAT
1106	K					36.1	36.1	N
1109	K					36.1	36.1	N
1113	J	0718						AAT
1113	J	0809						AAT
1114	K	0810		6.8	7.0	37.1	36.0	BM91,79,81a; AAT
1115	K	1225				36.1	36.1	N(C); AAT
1117	J	0626						AAT
1137	K	0913		7.0	7.2			BM79(NE of Aleppo),81a
1139	K	1012		7.3	7.4	36.1	37.1	BM91; PT(X-XI)
1151	J	0928		6.0	6.2	32.6	36.7	BM79,81a; N; PT(VIII); AAT
1156	G	1005						PT(IX-X)
1157	B	0715		5.9	6.1	34.5	36.5	BM79,81a; PK(VIII); N(1155,C)
1157	G	0815	010000	7.2	7.3	35.1	36.3	AB(C); BM79(M),91(Aug.12; ≠C),81a; AJ(≠C); AAT
1160	J			5.9	6.1	32.0	35.3	BM79,81a; N(C); AAT
1170	K	0629	010000	7.4	7.5	35.9	36.4	AB(C); B; BM91(M), 79,81a; AJ(≠C); PK(IX); AAT; PT(IX-X)
1182	J			6.5	6.7	32.6	36.7	BM79,81a; AAT; N(1183)
1183	B					34.5	36.5	N
1201	B	0602	040000	7.5		34.1	36.1	AB(C&M of 1202); BM79, 81b (Δf = 1000 km); N; AAT; PT(X-XI)
1202	J	0520	010000	6.8		32.5	35.5	BM79; N(C); AJ(≠C); PK(X); AAT
1203	B					33.3	35.2	N
1212	A	0502						PT(VIII-IX)
1284	B					33.3	36.2	N(C); PT(IX-X)
1287	G			7.0	7.2			BM91,79,81a; PK(VI); PT(VIII-IX)
1293	J	0111				32.0	34.9	N(C); PT(VIII,1292)
1339	B			7.0		34.3	35.5	N(C); B(M); PK(IX); PT(VIII)
1343	B	0101				33.3	36.2	N(C); PT(IX)
1354	G					35.1	36.4	N
1402	G					35.0	37.0	N

Table I *(continued)*.

Year	Zone	Date	Time	M_S	M_L	Lat.	Long.	References and remarks
1404	K	0222	010000	5.9	6.1	35.9	36.3	AB; BM81a; PT(IX)
1407	G	0429	010000	7.0		35.7	36.3	AB; B; BM91; N(C36; 36)
1408	K	1229		7.2	7.3	35.9	36.3	AM2; AJ; BM91; PK(IX); B; PT(X-XI); N(C35.1; 36.8)
1457	J							AAT(1456 or 1459)
1546	J	0114	110000	6.0		32.0	35.3	AK; BM79,81a(7.0L); PK(VI); AAT; N(7.0)
1588	A	0114						PT(IX)
1640	B							PK(VI)
1656	G	0200		6.8	7.0	34.9	36.2	BM79,91,81a; PK(VII); N(C34.3; 35.5)
1712	J	0616	050000					AAT
1752	A					31.2	34.2	N
1752	G	0621				35.0	36.0	N
1759	B					34.3	35.5	N
1759	J	1030	034500	6.6		33.1	35.6	AB; BM79,81a(6.5L); PK(VIII); AAT(X); PT(X-XI); N
1759	B	1125	192300	7.4		33.7	35.9	AB; AJ; BM79,91,81a(6.8L); PK(X)
1796	G	0426	010000	6.6		35.7	36.0	AB; AJ; BM81a(6.1L); N(C35.2; 35.8)
1802	B			6.0	6.2	34.0	36.2	BM79,81a
1810	B							PK(VII)
1822	K	0813	010000	7.4		36.7	36.9	AB; AJ(≠C); BM91(7.2L),79,81a(7.1L); N(C36; 36)
1834	A	0523	040000	6.1	6.3	31.3	35.6	BM91(M),79,81a; AAT; N
1837	J	0101	143400	7.0		33.0	35.5	A2; AJ(≠M&C); BM79,91,81a,b(6.4); N(6.4); PK(IX)
1838	J					32.0	34.5	N
1872	K	0403	074536	7.2		36.4	36.5	AB; AJ; BM79,91,81a(7.3L); N(7.5)
1902	J	0309	230500	5.5		31.8	35.2	K
1902	J	0329	223000	5.6		32.2	35.4	K
1903	J	0329	230000	5.2	5.5	32.0	35.5	BM79; BMA; PK(6; Io = VIII); AAT; N
1924	J	0227	202420	5.5		33.0	36.0	CP; A(4.8); BM79; BMA(5.0ML); PK(5.8); AAT
1927	J	0711	130355	6.0		32.0	35.4	AM; CP(6.1); BM79,91; BMA; AAT; PK(7.2,C31.9; 35.8); N
1928	J	0222	175048	5.5		32.0	35.5	CP; BM79; BMA(5.0L); PK(4.6); AAT
1936	K	0614	170134	5.5		36.5	36.0	CP
1951	K	0408	213805	5.8		36.6	36.1	CP; K(M5.7; C36.5; 35.7)
1952	K	1022	170000	5.0		36.5	35.3	N
1953	K	0324	211732	5.1		37.0	37.0	CP
1954	A	0913	214631	5.0		30.8	35.5	CP; BM79 (5.0L); BMA(4.5L); PK(5.2,C-; 36.0); AAT
1956	B	0316	193240	6.0		33.6	35.5	CP; BM79; BMA; PK(C; 5.5); A1(M4.8); AAT; N

Table I (*continued*).

Year	Zone	Date	Time	M_S	M_L	Lat.	Long.	References and remarks
1956	B	0316	194328	5.7		33.6	35.5	CP; PK(C; 5.8); A1(5.1); BM79; BMA
1956	J	1218	175303	5.6		31.6	35.5	CP; BM79; BMA(4.8L; C31.3; 35.6); PK(5.7); AAT
1971	K	0629	090812	5.0		37.1	36.8	ISC; CP(5.2)
1971	K	0711	201256	5.0		37.2	36.8	ISC; CP(5.3)
1971	K	0817	042933	5.0		37.1	36.8	ISC; CP
1979	A	0423	130156	5.0		31.2	35.5	ISC; BM79; BMA; AAT
1984	J	0824	060222	5.1		32.8	35.0	ISC
1997	B	0326	042251	5.6		33.4	35.5	MLJER
1997	B	0326	132021	5.0		33.7	35.5	MLJER

1) Historical earthquakes: $M \geq 5.9$. 20th century instrumentally recorded earthquakes: $M \geq 5.5$ (1900-1910); ≥ 5.0 (1910-1997).

2) A, J, B, G, and K are the respective designations of Araba, Jordan, Beqa'a, El-Ghab and Karasu seismogenic zones.

3) The first two digits represent the month, and the third and fourth digits show the date; 00 – unknown date.

4) Every two digits represent a value; from left to right: hours, minutes and seconds; 00 – unknown minutes and seconds.

5) All M_L values are taken from papers authored or co-authored by A. Ben-Menahem. These values were used to calculate M_S.

6) A1 - Ambraseys (1992); A2 - Ambraseys (1997); AB - Ambraseys and Barazangi (1989); AJ - Ambraseys and Jackson (1998); AK - Ambraseys and Karcz (1992); AM - Ambraseys and Melville (1988); AM2 - Ambraseys and Melville (1995); AAT - Amiran *et al.* (1994); BM79 - Ben-Menahem (1979); BM81a - Ben-Menahem (1981a); BM81b - Ben-Menahem (1981b); BM91 - Ben-Menahem (1991); BMA - Ben-Menahem and Aboodi (1981); B - Beydoun (1997); CP - Comninakis and Papazachos (1978); G - Guidoboni (1989); ISC - International Seismological Center; K - Karnik (1969-1970); MLJER - Local Magnitude of Jerusalem Observatory; N - (NEIC) National Earthquake Information Center; PK - Plassard and Kogoj (1981); PT - Poirier and Taher (1980) (only earthquakes with intensities larger than VII were taken); TSP - Tsapanos *et al.* (1990).

7) Semi-colons separate the references and their relevant remarks that are given between brackets. Most of the information, especially year, date and time, was taken from the first reference(s) in the list; when (M) or (C) follow a reference, this means that the given magnitude or coordinates were taken from this reference, respectively. When the information given in the catalogue are different from the data of the reference concerned, then: (6.5 or 5.5 L) – surface or local magnitude; (361 or large integer number) – year of occurrence; (C-; 36.8) – coordinates «longitude»; (D) – different date. Moreover, (X) and (f = 1000 km) – intensity and the average diameter of the area, over which the event was felt, respectively.

Table II. Information on the low and high seismic activity periods along DSTF. The first column gives the time period and the second column gives its duration. The number of events with $M_S \geq 6.3$ is shown in the third column while the mean return period for earthquakes with $M_S = 6.3$ is given in the fourth colum.

Years	Duration (year)	Events with $M_S \geq 6.3$	$T_{6.3}$ (years)	Remarks
184 B.C.-526	710	11	65	Quiescent period
526-587	61	6	10	Active period
587-1033	446	6	74	Quiescent period
1033-1202	169	12	14	Active period
1202-1759	557	5	111	Quiescent period
1759-1872	113	5	23	Active period

It also shows that the last strong event (M_s = 7.0) occurred in 1837. Table I also shows that the largest earthquake in the area of Wadi Araba and southern Dead Sea occurred in 362 (M_s = 6.5) while the last relatively strong earthquake (M_s = 6.1) occurred in 1834.

4. Segmentation of the Dead Sea Transform Fault

Figure 3 is a map of the Eastern Mediterranean region showing the extension of the DSTF and some fault branches. It also shows the location of the epicenters of earthquakes with assigned magnitudes and coordinates, for the periods: 1-1900 with $M_s \geq 5.9$; 1900-1910 with $M_s \geq 5.5$; and 1910-1998 with $M_s \geq 5.0$ (table I). The longitudinal extent of the five seismogenic zones into which the broader DSTF area has been divided on the basis of the geometry, geomorphology, structural geology and historical seismicity, is also shown. These zones are: Araba, Jordan, Beqa'a, El-Ghab and Karasu.

1) *The Araba segment* extends along Wadi Araba and the SE part of the Dead Sea between 29.5°-31.3°N for about 210 km. It trends in an almost straight SSW-NNE direction. In addition to the fact that historical records do not mention destructive earthquakes along this segment, which covers a sparsely populated area, the relatively low seismic activity is indicated by the instrumental record (Ben-Menahem, 1981a; Ben-Menahem and Aboodi, 1981).

2) *The Jordan valley segment* extends along the central and northern parts of the Dead Sea to the Huleh depression between 31.3°-33.1°N for about 200 km. It trends S-N in an almost straight direction. Its northern end coincides with the zone where the DSTF bifurcates into the Lebanese fault branches Yammouneh, Roum, Serghaya and other fault branches. On the other hand, in a more recent regionalization (Ben-Menahem, 1991), the northern limit of the Araba-Dead Sea and Jordan River region was put at 33.4°N. Tectonically, this segment is characterized by the pull-apart basins of the Dead Sea and Lake Tiberias, and has suffered several historical destructive earthquakes. At present, it is considered to be of relatively moderate seismicity (Ben-Menahem, 1981a). However, Rotstein (1987) dividing the Jordan valley into two zones (northern and southern zone), concluded that the northern zone has high probability for the generation of a strong earthquake during the next 50 years.

3) *The Beqa'a segment* extends along the western margin of the Beqa'a plain, following the Yammouneh-fault trend, between 33.1°-34.5°N for about 170 km. It trends SSW-NNE with very open curving. The northern end of this segment is at the site where the trend of the DSTF changes from SSW-NNE to S-N. Geomorphologically, this segment is characterized by the highest mountain elevations along the whole zone, and some compressional (due to transpression) structures. The historical record shows numerous very destructive earthquakes in this area, such as the 551, 1202, and 1759 (Plassard and Kogoj, 1981; Ambraseys and Melville, 1988; Ambraseys and Barazangi, 1989; Beydoun, 1997). Although Ben-Menahem (1981a) considered this zone almost as moderately active as the Jordan segment, its strong historical seismic record indicates that it is more active.

4) *El-Ghab segment* extends along the eastern flank of the Syrian coastal mountain range, along the Safita-fault trend in the south and El-Ghab pull-apart basin in the north, between 34.5°-35.8°N latitude for about 145 km. It trends S-N in an almost straight direction. Tectonically, this segment is characterized by the El-Ghab graben, which is considered by many investigators as a pull-apart basin (Radwan *et al.*, 1992). Although the historical record indicates that in the area of this segment very destructive earthquakes have occurred, this could be due to events outside the area of the segment. In fact, all earthquakes studied by Ambraseys and Barazangi (1989) with epicenters located in this area had magnitudes $M_s \approx 7.0$ or more. However, stronger events with magnitudes $M_s \approx 7.4$ and more were originated either to the south, or to the north of the area. Therefore, this segment is considered to be of moderate seismicity.

5) *Karasu segment* extends, together with the East Anatolia Fault, along the Karasu valley in SE Turkey between 35.8°-37.3°N. In this segment the Dead Sea Transform Fault merges

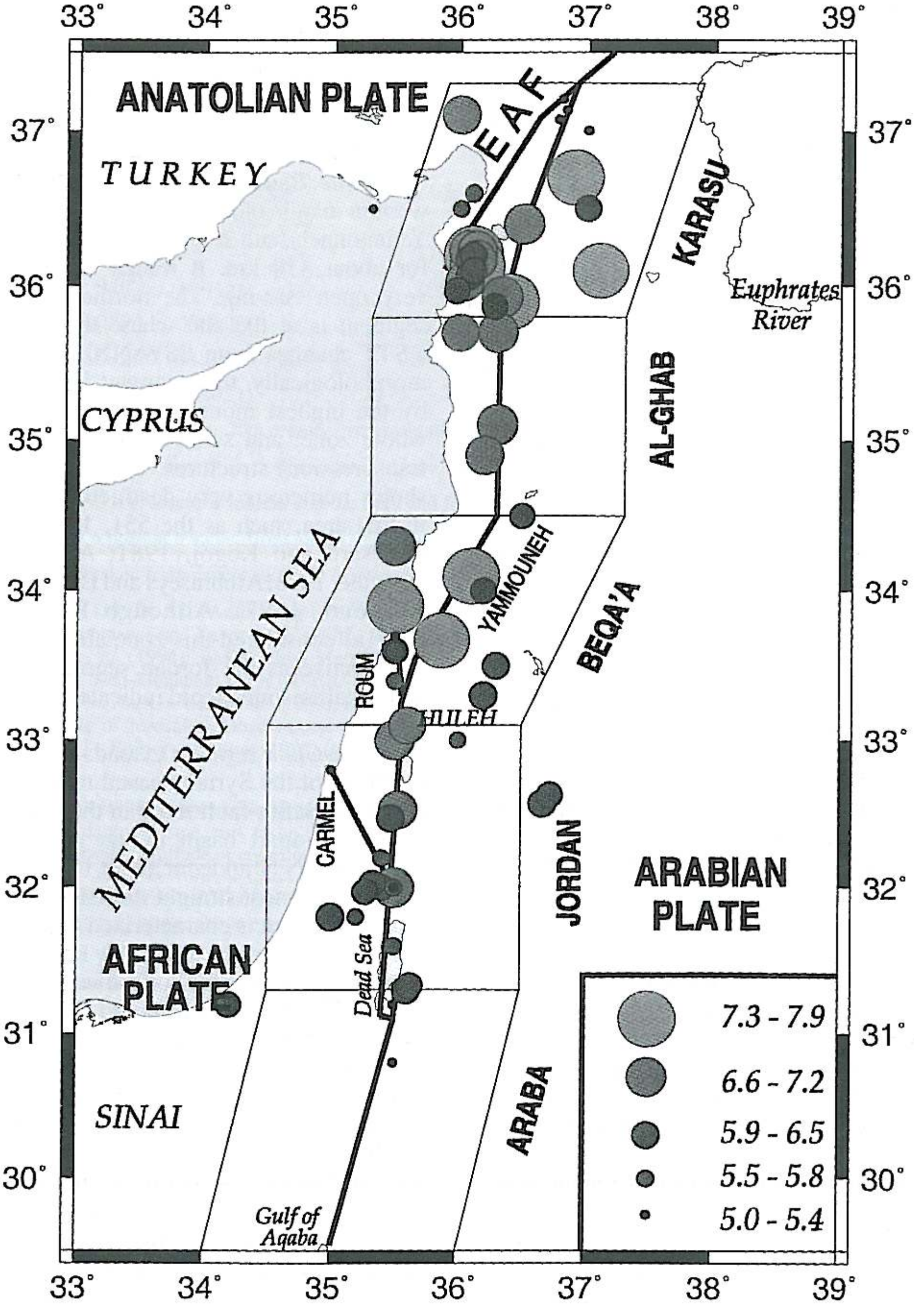

Fig. 3. Map of the Eastern Mediterranean region showing the Dead Sea Transform Fault and the epicenters of earthquakes for the periods: 0-1900 with $M_s \geq 5.9$; 1900-1910 with $M_s \geq 5.5$; and 1910-1998 with $M_s \geq 5.0$. The five seismogenic regions in which the area has been divided, are also shown.

with the Eastern Anatolian fault for about 170 km, in a SSW-NNE direction with wide open curving. Tectonically, the area of this segment is very complicated because it constitutes, in its northern part (Golbasi basin), the meeting point of the African plate to southwest, the Arabian plate to the east and southeast, and the Anatolian plate to the north and northwest. Historical seismic records show that this area is the most active along the DSTF, as it has accomodated very destructive earthquakes. This is because the southwestern segment of the East Anatolian fault passes through this area as well. Therefore, the high seismic activity is due, most probably, not only to the Karasu segment, but also to the southwestern segment of the East Anatolian Fault.

5. Time dependent seismicity

Searching for seismicity patterns along the DSTF, Papazachos *et al.* (1997a) identified two seismogenic regions in this area, which correspond to the segments south and north of 34.7° north latitude. By using the regional time- and magnitude predictable seismicity model it was found that the probabilities for the generation of strong ($M_S \geq 6.5$) earthquakes for the time interval 1993-2002 in these segments were low (0.13 and 0.22, respectively). An attempt is made in the present paper to re-examine the time dependent seismicity in this area, since new zonation is proposed and a new catalogue is used by applying this model (Papazachos, 1989; Papazachos and Papaioannou, 1993).

As it is known, the time predictable model (Bufe *et al.*, 1977; Shimazaki and Nakata, 1980; Sykes and Quittmeyer, 1981) suggests that the interevent times of large earthquakes in simple plate boundaries or single faults are proportional to the displacement of the preceding large events. Recent work on the repeat times of strong earthquakes indicated that the interevent time for a seismogenic region, which includes the main fault where the largest earthquakes occur and other smaller faults where smaller earthquakes occur, also increases with the magnitude of the preceding mainshock (Papazachos, 1989, 1993). Further work on mainshocks which occur in the continental fracture system led to a model which is expressed by the two relations that give the repeat time, T_t, and the magnitude, M_f, of the following mainshock in a certain region as a function of: the magnitude, M_{min}, of the smallest mainshock considered, the magnitude, M_p, of the preceding mainshock and the moment rate, m_0 (per year) in this region. By the application of a technique (Draper and Smith, 1966; Weisberg, 1980) which is widely used for the solution of similar problems and with a data set consisting of 1811 observations (T, M_{min}, M_p, M_f) the following empirical relations were found (Papazachos *et al.*, 1997b):

$$\log T_t = 0.19\, M_{min} + 0.33\, M_p - 0.39 \log m_0 + q \qquad (5.1)$$

$$M_f = 0.73\, M_{min} - 0.28\, M_p + 0.40 \log m_0 + m \qquad (5.2)$$

The parameters q and m must be determined by the available data in each case. The application of the model includes zonation, determination of the annual seismic moment release and declustering of the complete data sample, examination of the time distribution of mainshocks, determination of the parameters q and m of relations (5.1) and (5.2) and calculation of the model probabilities. Detailed discussion on these topics can be found in Papazachos *et al.* (1997a,b). The basic tenet of this model, which is called *regional time – and magnitude – predictable seismicity model*, is that the main factor which controls the duration of the mainshock interevent times in a certain region is the magnitude of the preceding mainshock. This is expressed by the positive value of the term 0.33 M_p in relation (5.1).

Table III lists the values of the parameters a and b' of the Gutenberg-Richter law (1944), M_{max} and $\log m_0$ for each of the five seismogenic regions of the area studied. A reliable b' value, equal to 0.86, was estimated for the whole DSTF area (Ben-Menahem and Aboodi, 1981; Ben-Menahem, 1991). By using this value and the completeness magnitude thresholds mentioned previously (part 4), the a values were determined.

Table III. Data of the five segments into which the DSTF has been divided. The first two columns give the names of the geographical coordinates of region vertices (north latitude, east longitude). Columns 3-6 give the parameters b' and a of the Gutenberg-Richter relation, the yearly seismic moment release rate m_0 and the maximum earthquake magnitude M_{max} observed in the region. The probabilities for the occurrence and the expected magnitudes for the next strong ($M \geq 6.0$) mainshocks in each seismogenic region of the Dead Sea Transform Fault area are given in the next two columns while the last two columns list the year of occurrence and the cumulative magnitude of the mainshocks of the region.

Seismogenic region	Coordinates vertices	b'	a	$\text{Log}\, m_0$	M_{max}	P_{10}	M_f	Year	M
Araba	29.5, 36.0	0.86	2.41	23.60	7.3	0.04	6.5	362	6.5
	29.5, 34.0							1834	6.1
	31.35, 34.5								
	31.35, 36.5								
Jordan	31.35, 34.5	0.86	3.03	24.16	7.2	0.06	6.8	658	6.4
	31.35, 36.5							746	7.2
	33.15, 36.5							1033	6.5
	33.15, 34.5							1159	5.9
								1202	6.8
								1546	6.0
								1759	6.6
								1837	7.0
								1902	5.8
								1924	5.5
								1927	6.0
								1956	5.6
Beqa'a	33.15, 34.5	0.86	3.10	24.40	7.5	0.07	6.9	551	7.5
	33.15, 36.5							844	6.4
	34.55, 37.3							991	6.5
	34.55, 35.3							1157	5.9
								1201	7.5
								1338	7.0
								1759	7.4
								1801	6.0
								1956	6.1
								1997	5.6
El-Ghab	34.55, 37.3	0.86	2.98	24.40	7.7	0.05	6.7	1157	7.2
	34.55, 35.3							1407	7.0
	35.8, 35.3							1656	6.8
	35.8, 37.3							1796	6.6

Table III (*continued*).

Seismogenic region	Coordinates vertices	b'	a	$\text{Log}\, m_0$	M_{max}	P_{10}	M_f	Year	M
Karasu	35.8, 35.3	0.86	3.36	24.90	7.9	0.05	7.1	37	6.3
	35.8, 37.3							115	7.3
	37.3, 37.9							340	6.0
	37.3, 35.9							457	6.3
								499	7.2
								528	7.1
								564	6.5
								713	6.8
								835	5.9
								859	7.9
								963	6.1
								971	5.9
								1114	6.8
								1139	7.3
								1170	7.4
								1404	5.9
								1408	7.2
								1822	7.4
								1872	7.2
								1936	5.5
								1951	5.8

The seismic moment rate, m_0 (dyne · cm yr^{-1}), expressing the tectonic loading exerted in the region, was calculated by a method proposed by Molnar (1979), that takes into account a and b' parameters as well as the magnitude M_{max} of the largest earthquake ever to occur in this region.

For the area under consideration 183 observations are available that can be considered a quite satisfactory data sample. The values of q and m parameters and the corresponding standard deviations are:

$$q = 8.16,\ \sigma_q = 0.40$$
$$\text{and } m = -5.53,\ \sigma_m = 0.45. \tag{5.3}$$

In addition to relation (5.1) the probability density function of the observed interevent time, T, to the calculated one, T_t, has to be defined in order to proceed in the determination of the model probabilities. Once this function is defined, earthquake repeat time estimates can be presented in terms of a conditional probability describing the likelihood of failure within a certain time interval $t + \Delta t$, provided that the event has not occurred during the time, t. Relation (5.2) can be used to estimate the magnitude of the expected mainshock in each seismogenic region.

The name and the geographic coordinates of the vertices of each seismogenic region are given in the first two columns of table III. The probabilities, P_{10}, and the magnitudes, M_f, of the expected mainshocks are given in the seventh and eighth columns, where the model probabilities, P_{10}, were calculated with M_{min} = 6.0. The year of occurrence and the cumulative magnitude of the main shocks, that is, the representative magnitude determined by summing up all seismic moments of the shocks of each seismic sequence (Papazachos *et al.*, 1997a,b), are given in the last two columns.

6. Discussion

The historical seismic record of the Dead Sea Transform Fault area indicates that large and destructive earthquakes have occurred in the past 2000 years (table I). The strongest events occurred in the Karasu and Beqa'a seismogenic zones (fig. 3). In the Karasu zone, the epicenters of the largest events are dispersed in a wide zone (about 100 km), and two of them were probably originated along the East Anatolian Fault rather than the Karasu segment of the Dead Sea Fault. The cluster of events between the two faults could be due to a fault branch bifurcating from the northern end of El-Ghab towards NNW similar to the branching of Carmel and Roum faults to the south (fig. 1). Chronologically, table I shows that the largest events $M_s > 7.2$ have occurred in long «swarms» with quiescent periods of about 450 to 700 years as Ambraseys and Barazangi (1989) also noticed. These periods of high seismicity have recurrence intervals of about 450-700 years. In the Beqa'a seismogenic zone, the epicenters of the largest seismic events are located along the Yammouneh fault, the main fault strand of the DSTF in Lebanon. Smaller events originated in a relatively broader zone, and especially along the Roum fault and its northern extension (fig. 1). Chronologically, from table I it is evident that the largest seismic events in this zone have recurrence intervals of 550 to 650 years. In the past 2000 years, each of the Jordan and El-Ghab seismogenic zones accommodated one earthquake with magnitude equal to 7.2. The second highest magnitude in both regions was 7.0 (table I). The uniqueness of these events and the skeptic approach towards historical seismic data suggest that these earthquakes (of M 7.2) may have been overestimated. However, in the application of the time- and magnitude-predictable model these events are considered as they appear in the table. The scarcity of seismic events, and the lack of earthquakes with $M_s > 6.5$, in the Araba zone indicates, as Ben-Menahem (1981a) also concluded, that this seismogenic region has low seismic activity and high aseismic slip. As for the whole region, the long recurrence rate of strong seismic events in all seismogenic zones is probably responsible for the scarce instrumental record in the 20th century.

From the preceding discussion, it is suggested that, in terms of seismicity, the Dead Sea Transform Fault seismogenic zones could be classified into three groups. The first group includes only the Araba zone, which is characterized by low seismic activity, and the absence of significant transtensional and transpressional features except for the southern part of the Dead Sea, which constitutes a transitional area into the Jordan zone. Therefore, the Arabian and African plates are probably sliding aseismically. The second group includes the Jordan-valley and El-Ghab zones. This group is characterized by left stepping, creating in left-lateral transform faults, pull-apart basins, which are found in both zones. This group is characterized by moderate seismic activity. The third group includes the Beqa'a and Karasu zones. Transpressional features due to the zones' diversion to the right are evident in this group, which is characterized by strong seismic activity.

Figures 2a,b, which depict the rate of seismic activity along the DSTF, also show that large swarms of earthquakes of varying magnitudes occurred three times during the 6th, 12th, and the end of 18th – beginning of 19th centuries with a recurrence period of 450-700 years. These long cycles of quiescence were disrupted during the middle of 4th and 9th centuries and the closure of 14th century. During the time interval 1408-1656 there was not any reported event with magnitude larger than 6.0. Although this interval falls within the 13th-18th century quiescent period, it might be artificially imposed by lack of historical descriptive records. However, the detection of 1546 (M = 6.0) earthquake in Palestine, suggests that very strong earthquakes could not be simply missed, even if they originated at relatively large distances from that area.

In contrast to different segmentations and regionalizations of Ben-Menahem (1981a, 1991) and Ben-Menahem and Aboodi (1981), this study takes into account the geometry, geomorphology and structural geology of the Dead Sea Transform Fault area together with historical seismicity. The instrumental record was not given a significant role in the zonation due to its scarcity which is, probably, inherited by the fact that the whole region is currently (20th century) passing through a seismically quiescent period. Hence, the segmentation results of this study can be considered reliable for any seismicity model studies, as well as for seismic hazard assessment.

7. Conclusions

The aforementioned results and discussion led to the following conclusions:

– The Dead Sea Transform Fault area is subdivided into five seismogenic zones, namely: 1) Araba segment extends along Wadi Araba and the southernmost part of the Dead Sea between the latitudes 29.5° and 31.3° N, and trends SSW-NNE; 2) Jordan-valley segment extends along the central and northern parts of the Dead Sea and the Jordan valley to the Huleh depression between the latitudes 31.3° and 33.1°N, and trends S-N; 3) Beqa'a segment extends along the western margin of the Beqa'a valley in Lebanon between the latitudes 33.1° and 34.5°N and trends SSW-NNE; 4) El-Ghab segment extends along the eastern flank of the coastal mountain range of Syria between the latitudes 34.5° and 35.8°N and trends S-N; 5) Karasu segment extends along the Karasu valley in SE Turkey between the latitudes 35.8° and 37.3°N and trends SSW-NNE.

– These seismogenic zones do not exhibit the same seismic activity: the Araba zone is characterized by low seismic activity, and the absence of transtensional and transpressional features; the Jordan-valley and El-Ghab zones, however, are characterized by moderate seismic activity and the presence of pull-apart basins; on the other hand, the Beqa'a and Karasu zones are characterized by high seismic activity (events with $M \geq 7.0$) and the presence of transpressional features.

– In the past two millennia, three large regional swarms of earthquakes of varying magnitudes occurred during the 6th, 12th, and the end of 18th and the beginning of 19th centuries with a recurrence period of about 600 years.

Acknowledgements

We acknowledge the grant of the American University of Beirut Research Board to the first author to visit the Geophysics Laboratory in the Aristotle University of Thessaloniki. Special thanks go to Professor B.C. Papazachos for his valuable remarks and discussion. We also thank Professors H. Eyidogan, A. Barka, R. Console and an anonymous reviewer for critically reading the manuscript and helpful suggestions for its improvement. The GMT system (Wessel and Smith, 1995) was used to plot figs. 1 and 3.

REFERENCES

AMBRASEYS, N.N. (1989): Temporal seismic quiescence: SE Turkey, *Geophys. J.*, **96**, 311-331.

AMBRASEYS, N.N. (1992): Reappraisal of the seismic activity in Cyprus: 1894-1991, ESEE Research Report, *Engineering Seismology*, No. 92/ 9.

AMBRASEYS, N.N. (1997): The earthquake of 1 January 1837 in Southern Lebanon and Northern Israel, *Ann. Geofis.*, **40** (4), 923-935.

AMBRASEYS, N.N. and M. BARAZANGI (1989): The 1759 earthquake in the Bekaa valley: implication for earthquake hazard assessment in the Eastern Mediterranean region, *J. Geophys. Res.*, **94**, 4007-4013.

AMBRASEYS, N.N. and J.A. JACKSON (1998): Faulting associated with historical and recent earthquakes in the Eastern Mediterranean region, *Geophys. J. Int.*, **133**, 390-406.

AMBRASEYS, N.N. and I. KARCZ (1992): The earthquake of 1546 in the Holly Land, *Terra Nova*, **4**, 253-262.

AMBRASEYS, N.N. and C.P. MELVILLE (1988): An analysis of the Eastern Mediterranean earthquake of 20 May 1202, in *History of Seismology and Earthquakes of the World*, edited by W.H. LEE (Academic, San Diego, California), 181-200.

AMBRASEYS, N.N. and C.P. MELVILLE (1995): Historical evidence of faulting in Eastern Anatolia and Northern Syria, *Ann. Geofis.*, **38** (3-4), 337-343.

AMIRAN, D.H.K., E. ARIEH and T. TURCOTTE (1994): Earthquakes in Israel and adjacent areas: macroseismic observations since 100 B.C.E., *Isr. Explor. J.*, **44**, 261-305.

BARAZANGI, M., D. SEBER, T. CHAIMOV, J. BEST, R. LITAK, D. AL-SAAD and T. SAWAF (1993): Tectonic evolution of the Northern Arabian plate in Western Syria, in

Recent Evolution and Seismicity of the Mediterranean Region, edited by E. MANTOVANI, A. MORELLI and E. BOSCHI, NATO ASI Series (Kluwer Academic, Dordrecht, the Netherlands), 117-140.

BARTOV, Y., G. STEINITZ, M. EYAL and Y. EYAL (1980): Sinistral movement along the Gulf of Aqaba – its age and relation to the opening of the Red Sea, *Nature*, **285**, 220-222.

BEN-MENAHEM, A. (1979): Earthquake for the Middle-East, 92 B.C.-1980 A. D., *Boll. Geofis. Teor. Appl.*, **21**, 245-310.

BEN-MENAHEM, A. (1981a): Variation of slip and creep along the Levant Rift over the past 4500 years, *Tectonophysics*, **80**, 183-197.

BEN-MENAHEM, A. (1981b): A seismicity cycle of 1500 years on the Dead-Sea Rift, *Boll. Geofis. Teor. Appl.*, **23**, 349-354.

BEN-MENAHEM, A. (1991): Four thousand years of seismicity along the Dead Sea Rift, *J. Geophys. Res.*, **96**, 20195-20216.

BEN-MENAHEM, A. and E. ABOODI (1981): Micro- and macroseismicity of the Dead Sea rift and off-coast Eastern Mediterranean, *Tectonophysics*, **80**, 199-233.

BEN-MENAHEM, A., E. ABOODI, M. VERED and R.L. KOVACH (1977): Rate of seismicity of the Dead-Sea region over the past 4000 years, *Phys. Earth. Planet. Inter.*, **14**, 17-27.

BEYDOUN, Z.R. (1997): Earthquakes in Lebanon: an Overview, *Leban. Sci. Bull.*, **10**, 109-129.

BUFE, C.G., P.W. HARSCH and R.O. BUDFORD (1977): Steady-state seismic slip: a precise recurrence model, *Geophys. Res. Lett.*, **4**, 91-94.

BUTLER, R.W.H., S. SPENCER and H.M. GRIFFITHS (1997): Transcurrent fault activity on the Dead Sea Transform in Lebanon and its implications for plate tectonics and seismic hazard, *J. Geol. Soc., London*, **154**, 757-760.

BUTLER, R.W.H., S. SPENCER and H. GRIFFITHS (1998): The structural response to evolving plate kinematics during transpression: evolution of the Lebanese restraining bend of the Dead Sea transform, in *Continental Transpressional and Transtensional Tectonics*, edited by R.E. HOLDSWORTH, R.A. STRACHAN and J.F. DEWEY, *Geol. Soc. London, Spec. Publ.*, **135**, 81-106.

CHAIMOV, T.A., M. BARAZANGI, D. AL-SAAD, T. SAWAF and A. GEBRAN (1990): Crustal shortening in the Palmyride fold belt, Syria, and implications for movement along the Dead Sea fault system, *Tectonics*, **9**, 1369-1386.

COMNINAKIS, P.E. and B.C. PAPAZACHOS (1978): A catalogue of earthquakes in the Mediterranean and surrounding area for the period 1901-1975, *Publication Geophysical Laboratory*, University of Thessaloniki, **5**, pp. 96.

DRAPER, N.A. and H. SMITH (1966): *Applied Regression Analysis* (Wiley, New York, NY), pp. 407.

DUBERTRET, M.L. (1932): Les formes structurales de la Syrie et de la Palestine, *C.R. Acad. Sci. France*, **195**, 66.

FREUND, R., Z. GARFUNKEL, I. ZAK, M. GOLDGERG, T. WEISSBROD and B. DERIN (1970): The shear along the Dead Sea rift, *Philos. Trans. R. Soc. London, Ser. A*, **267**, 107-130.

GARFUNKEL, Z. (1981): Internal structure of the Dead Sea leaky transform (rift) in relation to plate kinematics, *Tectonophysics*, **80**, 81-108.

GARFUNKEL, Z. and Y. BARTOV (1977): The tectonics of the Suez rift, *Geol. Surv. Isr. Bull.*, **71**, 44.

GARFUNKEL, Z., I. ZAK and R. FREUND (1981): Active faulting in the Dead Sea Rift, *Tectonophysics*, **80**, 1-26.

GIRDLER, R.W. (1990): The Dead Sea transform fault system, *Tectonophysics*, **180**, 1-13.

GUTENBERG, B. and C.F. RICHTER (1944): Frequency of earthquakes in California, *Bull. Seismol. Soc. Am.*, **34**, 185-188.

GUIDOBONI, E. (1989): *I Terremoti Prima del Mille in Italia e nell'Area Mediterranea. Storia Archeologia Sismologia*, Storia-Geofisica-Ambiente (SGA), Bologna, pp. 765.

HANCOCK, P.L. and M.S. ATIYA (1979): Tectonic significance of mesofracture systems associated with the Lebanese segment of the Dead Sea Transform fault, *J. Struct. Geol.*, **1**, 143-153.

HATCHER, R.D., I. ZIETZ, R.D. REGAN and M. ABU-AJAMIEH (1981): Sinistral strike-slip motion on the Dead Sea rift: Confirmation from new magnetic data, *Geology*, **9**, 458-462.

HOFSTETTER, A., T. VAN ECK and A. SHAPIRA (1996): Seismic activity along fault branches of the Dead Sea-Jordan transform system: the Camel-Tirza fault system, *Tectonophysics*, **267**, 317-330.

JOFFE, S. and Z. GARFUNKEL (1987): Plate kinematics of the cicum Red Sea – a re-evaluation, *Tectonophysics*, **141**, 5-22.

KARNIK, V. (1969-1970): *Seismicity of the European Area* (D. Reidel Publ. Co., Dordrecht, Holland), parts I-II.

KHAIR, K., G.N. TSOKAS and T. SAWAF (1997): Crustal structure of Northern Levant region: multiple source Werner deconvolution estimates for Bouguer gravity anomalies, *Geophys. J. Int.*, **128**, 605-616.

MOLNAR, P. (1979): Earthquake recurrence intervals and plate tectonics, *Bull. Seismol. Soc. Am.*, **69**, 115-133.

PAPAZACHOS, B.C. (1989): A time predictable model for earthquakes in Greece, *Bull. Seismol. Soc. Am*, **79**, 77-84.

PAPAZACHOS, B.C. (1993): Long-term prediction of intermediate depth earthquakes in Southern Aegean region based on a time-predictable model, *Natural Hazards*, **7**, 211-218.

PAPAZACHOS, B.C. and CH.A. PAPAIOANNOU (1993): Long-term earthquake prediction in the Aegean area based on a time and magnitude predictable model, *Pure Appl. Geophys.*, **140**, 593-612.

PAPAZACHOS, B.C., G.F. KARAKAISIS, E.E. PAPADIMITRIOU and CH.A. PAPAIOANNOU (1997a): The regional time and magnitude predictable model and its application to the Alpine-Himalayan belt, *Tectonophysics*, **271**, 295-323.

PAPAZACHOS, B.C., E.E. PAPADIMITRIOU, G.F. KARAKAISIS and D.G. PANAGIOTOPOULOS (1997b): Long-term earthquake prediction in the Circum-Pacific convergent belt, *Pure Appl. Geophys.*, **149**, 173-217.

PLASSARD, J. and B. KOGOJ (1981): Seismicite du Liban, *Annales-Memoires de l'Observatoire de Ksara*, V.4 (Seismologie) cah. 1, third edition, p. 67 CNRS, Beyrouth.

POIRIER, J.P. and M.A. TAHER (1980): Historical seismicity in the Near and Middle East, North Africa, and Spain from Arabic documents (VIIth-XVIIth Century), *Bull. Seismol. Soc. Am.*, **70**, 2185-2201.

QUENNELL, A.M. (1959): Tectonics of the Dead Sea rift, in *20th Inter. Geol. Congr. Proc., Mexico, 1956*, ASGA, 385-403.

QUENNELL, A.M. (1984): The Eastern Arabia rift system, in *The Geological Evolution of the Eastern Mediterranean*, edited by J.E. DIXON and A.H.F. ROBERTSON, *Geol. Soc., Spec. Publ.*, **17**, 775-788.

RADWAN, Y., H. AL-NAJJAR and I. LAYOUS (1992): Indications of new tectonics along the Syrian Lebanese fault (El-Ghab depression), in *The Proceedings of the Regional Workshop on Archaeoseismicity in the Mediterranean Region, Damascus*, 122-133.

ROTSTEIN, Y. (1987): Gaussian probability estimates for large earthquake occurrence in the Jordan Valley, Dead Sea rift, *Tectonophysics*, **141**, 95-105.

SALAMON, A., A. HOFSTETTER, Z. GARFUNKEL and H. RON (1996): Seismicity of the Eastern Mediterranean region: perspective from the Sinai subplate, *Tectonophysics*, **263**, 293-305.

SHAPIRA, A. and L. FELDMAN (1987): Microseismicity of three locations along the Jordan Rift, *Tectonophysics*, **141**, 89-94.

SHIMAZAKI, K. and T. NAKATA (1980): Time-predictable recurrence model for large earthquakes, *Geophys. Res. Lett.*, **7**, 279-282.

SYKES, L.R. and R.C. QUITTMEYER (1981): Repeat times of great earthquakes along simple plate boundaries, in *Earthquake Prediction*, an *International Review*, edited by D.W. SIMPSON and P.G. RICHARDS, *Maurice Ewing Series, AGU*, **4**, 217-247.

TSAPANOS, T.M., E.M. SCORDILIS and B.C. PAPAZACHOS (1990): A global catalogue of strong earthquakes ($M \geq 5.5$) during the time period 1966-1985, *Publication Geophysical Laboratory*, University of Thessaloniki, **10**, pp. 90.

VAN ECK, T. and A. HOFSTETTER (1990): Fault geometry and spatial clustering of microearthquakes along the Dead Sea-Jordan rift fault zone, *Tectonophysics*, **180**, 15-27.

WEISBERG, S. (1980): *Applied Linear Regression* (Wiley, New York, NY), pp. 283.

WESSEL, P. and W.H.F. SMITH (1995): New version of the Generic Mapping Tools released, *Eos Trans. Am. Geophys. Un.*, **76**, pp. 329.

ZAK, I. and R. FREUND (1966): Recent strike-slip movement along the Dead Sea rift, *Isr. J. Earth. Sci.*, **15**, 33-37.

(received November 16, 1998;
accepted November 12, 1999)